Tropical Wetland Journal
Journal homepage: twj.ulm.ac.id | Published by Postgraduate Program - Lambung Mangkurat University | e-ISSN: 2654-279X

Original article
DOI 10.20527/twj.v9i1.116

Removal of Turbidity and Color of Contaminated Drinking Water Sources using Chitosan-Bentonite Composite as Adsorbent

Chairul Irawan*, Iryanti Fatyasari Nata, Meilana Dharma Putra, Maulana Wahyu Noor Ramadhan.

Department of Chemical Engineering, Faculty of Engineering, Lambung Mangkurat University, Banjarbaru 70714, South Kalimantan, Indonesia

* Correspondence: cirawan@ulm.ac.id; Tel.: +62-511-473-858

Received: May 05, 2023; Accepted: October 30, 2023 ; Published: November 22, 2023

ABSTRACT

The composites of biopolymer chitosan obtained from the swamp fish scale with bentonite as clay minerals has been characterized by the structural, mechanical, surface functional group and composition properties using scanning electron microscopy (SEM), thermal gravimetric analysis (TGA), X-ray fluorescence (XRF) and X-ray Diffraction (XRD) analysis. The morphology structure obtained by SEM for the original chitosan, bentonite, and its composites showed that the particles are relatively well dispersed in the chitosan matrix. The physicochemical properties of the chitosan-bentonite composites depend significantly on the chemistry of the polymer matrices, the nature of bentonite, their modification, and the preparation methods that showed by SEM, TGA, XRF and XRD analysis. The obtained composite of chitosan bentonite was then applied for treating raw water sources of drinking water in Bilu river, South Kalimantan, during the dry season. The raw water sources contained a high value of turbidity (ca. of 370±30 NTU) and color (1300±150 Pt-Co). Batch experiment using the composite of chitosan bentonite for treating raw water sources was significant to reduce the value of turbidity, and the color becomes 24.8±2 NTU and 86.7±5 Pt-Co, respectively. The results then compare to the treatment using the commercial chitosan and bentonite self. Moreover, it found that the raw water treatment using the composite of chitosan-bentonite is more favorable than chitosan and bentonite materials.

Keywords: Adsorption, Bentonite, Chitosan Composite, Contaminated Drinking Water Sources.

1. Introduction

The occurrence of contaminated raw water from an anthropogenic source in the surface water increases in a continuous and parallel way with increased population and industrial development. Contaminated raw water will have a potential adverse health effect on humans and other living things when supplied to Municipal Waterworks for drinking water. Therefore, the raw water supplied should first be treated to ensure that it is safe to consume as drinking water and free from endangering materials and microorganisms. It has received a growing attention approach to mitigating water-related health risks and reducing chemical and treatment costs [1]. In this case, Bilu river in South Kalimantan as raw sources water of Municipal Waterworks, called PDAM Bandarmasih, in the dry season contains a high value of turbidity (ca. of 370±30 NTU) and colour (1300±150 Pt-Co).

Treatment of contaminated raw water could be achieved by several methods, such as chemical precipitation, ion exchange, adsorption, membrane filtration, reverse osmosis, disinfection, sedimentation and coagulation–flocculation processes [2–4]. Although many treatment processes have

been utilized for contaminated raw water, however, it still requires the possibility of cost-effective and efficient treatment approaches that renders the contaminated raw water, while avoiding the adverse effects on the treated system using natural adsorbent such as biomass waste [5, 6].

Currently, some researcher develops biocomposites based on biopolymers and clay minerals, which are low costly, biocompatibility, biodegradability, absence of toxicity, and highly efficient, which have attracted considerable attention accounting to their thermal stability, functional properties, and structure [7–10]. Chitosan has been studied extensively for application water treatment [11–14], but mechanical and water barrier properties of chitosan itself should be improved [15]. Chitosan is derived by alkaline N-deacetylation of chitin from crab, shrimps, shellfish, and another crustacean [16–19]. An interaction between chitosan and clay (montmorillonite) was investigated and resulted the enhancement of tensile strength, thermal stability, and water barrier properties of chitosan in addition MMT, significantly [15, 20, 21]. Bentonite is the most preferred clay, which is fine-grained inorganic clay of the mineral montmorillonite [22, 23].. Bentonite was also has a negative charge that important for adsorbing the cation contaminant in water [24].. Since similar research seems had been done before, however, nevertheless the researcher investigated chitosan from fish scales composite with bentonite as clay minerals, then applied for raw water sources, especially for turbidity and color adsorption. In this research, clay composites were prepared from bentonite clay with chitosan from fish scales using a chemical precipitation process. Chitosan that used in this research was made by using a local fish scale, called papuyu (Anabas testudines Bloch) as the based material for chitin. This present work aims to experimentally investigate the treatment of contaminated raw water by using chitosan-bentonite composites as adsorbent. This research was also to evaluate the effectiveness of chitosan–bentonite composites for the efficiency and capacity of turbidity and color removal, to determine the optimal conditions for the adsorption process, and then compared the result of chitosan and bentonite and its self as a natural adsorbent for the contaminated raw water treatment.

2. Materials and Methods

Materials

Raw sources water samples taken from Bilu river, South Kalimantan, in the dry season (March–June). Turbidity parameter (in NTU) is checked by using U-50 Horiba series Multi-parameter water quality checker, while the color (in Pt-Co) identified by UV-Vis photometer. Authors well prepared chitosan from fish scales, 1 wt % in 1% acetic acid at room temperature with a deacetylation degree of 90–96%. The bentonite, glacial acetic acid, and others chemicals were pure grade analytical obtained from Aldrich and used without further purification.

Methods

Synthesis of chitosan–bentonite composites

Preparation of chitosan bentonite was adopted with modified a method described by [15]. Aqueous solutions of 1.0 wt.% were prepared by dissolving chitosan powder in acetic acid solution (1 wt.%). The powders of bentonite as clay minerals (3% based on chitosan) were dispersed in 100 ml of 1% acetic acid solution and stirred for 24 h at room temperature. Then, chitosan solution was added slowly to the bentonite dispersion. The obtained mixtures were vigorously stirred for 24 h at room temperature (150 rpm). The solution composites were poured on the glass plate covered with polyethylene film and evaporated at room temperature. The obtained composite, called chitosan bentonite (Ch-B), was then dried at 60oC, 8 h into the oven. The structure morphology properties, thermal behavior, and chemical composition properties of chitosan-bentonite composites Ch-B, chitosan, and bentonite have been characterized using scanning electron microscopy (SEM), thermogravimetric analysis (TGA), X-ray fluorescence (XRF) and X-ray diffraction (XRD). The surface morphology of the composite, chitosan and bentonite were observed by Scanning electron microscopy (SEM, JOEL JSM-6500F) with energy-dispersive X-ray spectroscopy (EDAX), TG-HDSC LINSEIS STA Platinum Series (simultaneous thermal analysis) used to determine simultaneous changes of mass (TG) and energetic effects (DTA/DSC), and Elemental Analysis by Energy Dispersive X-ray Fluorescence (PANalytical's MiniPal 4 energy-dispersive EDXRF bench-top spectrometer) to conclude the identity and quantities of the elements in samples. The X-ray diffraction (XRD) measurement was performed on Rigaku D/MAX-B X-ray diffractometer by using Copper K-alpha (CuK□) radiation. The operation voltage and current were kept at 40 kV and 100 mA, respectively.

Batch Adsorption Experimental of Contaminated Raw Water

Batch adsorption experiments were carried out by putting 100 mL of raw water in 250-mL plastic bottles and adjusting its pH values with sodium hydroxide (NaOH, 1M) and nitric acid (HNO_3, 1M). A weighted amount of the adsorbent (Ch-B) was then added into a plastic bottle. The mixture was placed in a shaker with a water bath at a predetermined temperature for a certain time. At the end of the experiment, the solution was centrifuged and filtered by using a 0.2 μm PVDF membrane. Finally, the filtrates were analyzed for residual turbidity and color concentration. Turbidity was measured by Hach 2100Q Portable Turbidimeters and the color was analysis using PFX-995/P Colorimeter testing Pt-Co color, DC Scientific. Adsorbed turbidity and color were calculated from the difference between the initial and equilibrium concentrations. The adsorption experiments were done in triplicate samples and the average value was taken. The effect of contact time, adsorbent dose, and equilibrium pH on the adsorption processes were also studied. Adsorption experiments for the studied effect of adsorbent dose and equilibrium pH were always performed after the adsorption equilibrium reached around 180 min. All adsorption experiments were conducted at room temperature around 25±2°C. The adsorption isotherm plots were constructed from the q_e versus C_e data points. The parameter q_e is the equilibrium amount of adsorbate adsorbed, and C_e is the residual amount of adsorbate at equilibrium. The value of q_e is calculated based on Equation (1) as follows:

$$q_e = \frac{C_0 - C_e}{m} \; x \; V \qquad (1)$$

where C_0 is the initial concentration of adsorbate, m (g) is the mass of the adsorbent, and V (L) is the total volume of the adsorption system.

The result of composite adsorbent was used then compared to the chitosan and bentonite itself as adsorbents. The data from the experiment were fitted and figured out by Sigma Plot® version 10 of software.

3. Results and Discussion

Physicochemical properties of Chitosan, Bentonite, and Chitosan-Bentonite Composite

Fig. 1 is shown SEM microphotographs of the surface morphology of chitosan, bentonite, and chitosan–bentonite composite (Ch-B). It was observed chitosan (Fig. 1a.) appears to have fibrillar and granular structure on the surface while the surface is relative smoother and the structures of the fiber are seen on a fractured appearance. It was also shown that the chitosan from the fish scale has become porous and fibril structures [20, 25]. Bentonite structures are relatively flat and quite smooth, seeming composed of a single plate as shown in Fig. 1b. In the case of the chitosan composite with bentonite, it seems the fibril of chitosan agglomerates on a plate of bentonite, while the surface is smooth (Fig. 1c).

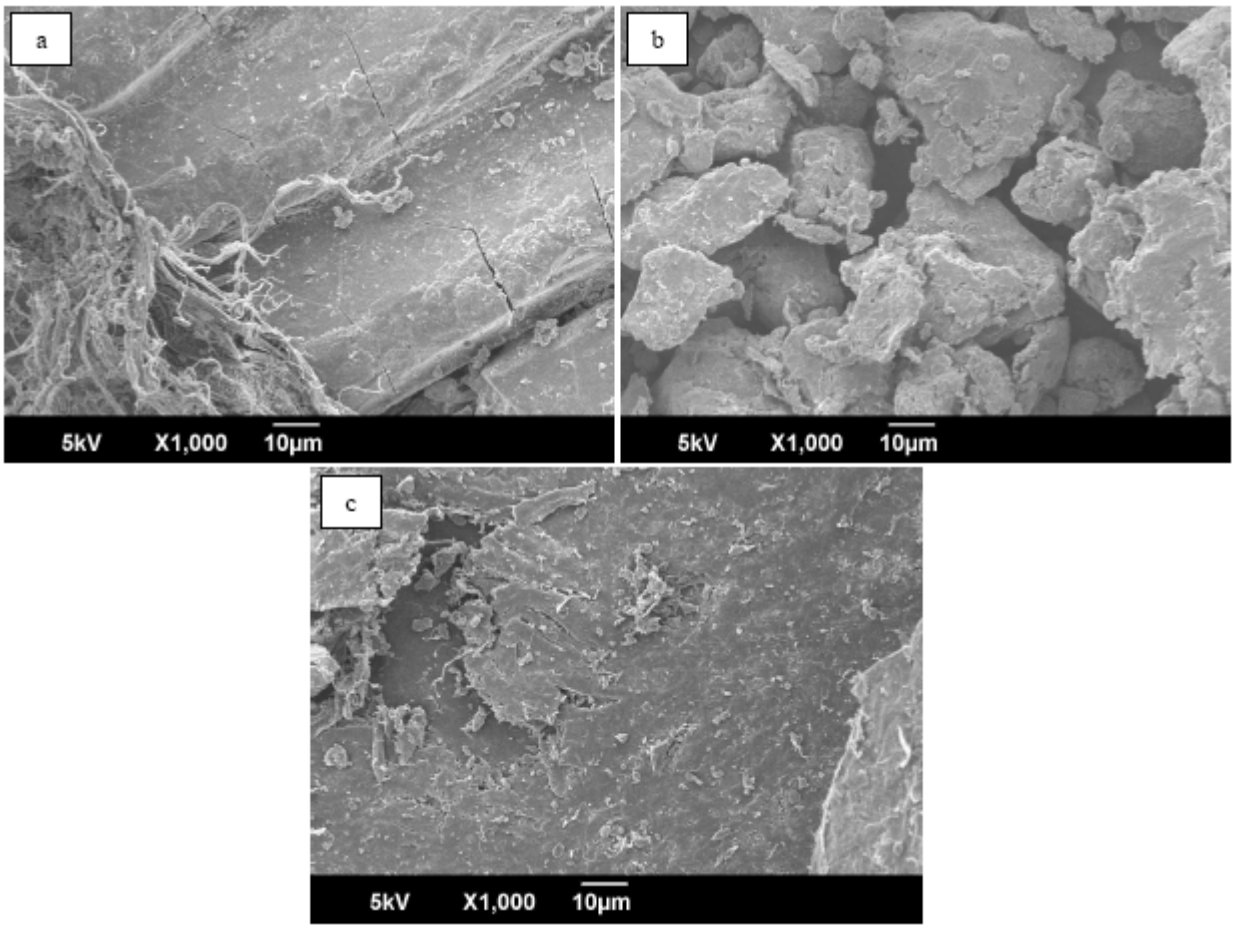

Fig. 1. SEM surface morphology images of (a) Chitosan, (b) Bentonite, and (c) Ch-B Composite

Thermal stability of chitosan, bentonite, and Ch-B composites was analyzed by thermogravimetric analysis under nitrogen flow as shown in **Fig. 2**. Thermal properties of polymer composite provide a valuable evidence conditions regarding the stability and improvement of properties oh polymer composite with other compounds [26]. The TGA curve of the chitosan sample shows a weight loss in two stages. The first stage (30–200^{o}C) is associated with the loss of absorbed and bound water and residues of acetic acid compounds [26] and shows around 6.6 % loss in weight. The second stage (200–600^{o}C) is due to the degradation of chitosan, and during this process, there was about 42.1% loss in weight. Bentonite and Ch-B composite was more thermally stable than chitosan, as indicated by the appearance of a peak at a higher temperature.

The bentonite could be found in three peaks of TG curve. The TGA of bentonite shown in the first stage, a smaller loss in weight (9%), was observed than in the second stage (11%) and three stages (17%). The TGA of Ch-B composite can find two peaks in TG curve, shown in the first stage a smaller loss in weight (15.9%) was observed than in the second stage (29.1%). This difference is associated with the modification of the surface by organic compounds. Besides of bentonite into chitosan provides a thermal barrier and decreases the weight loss [26].

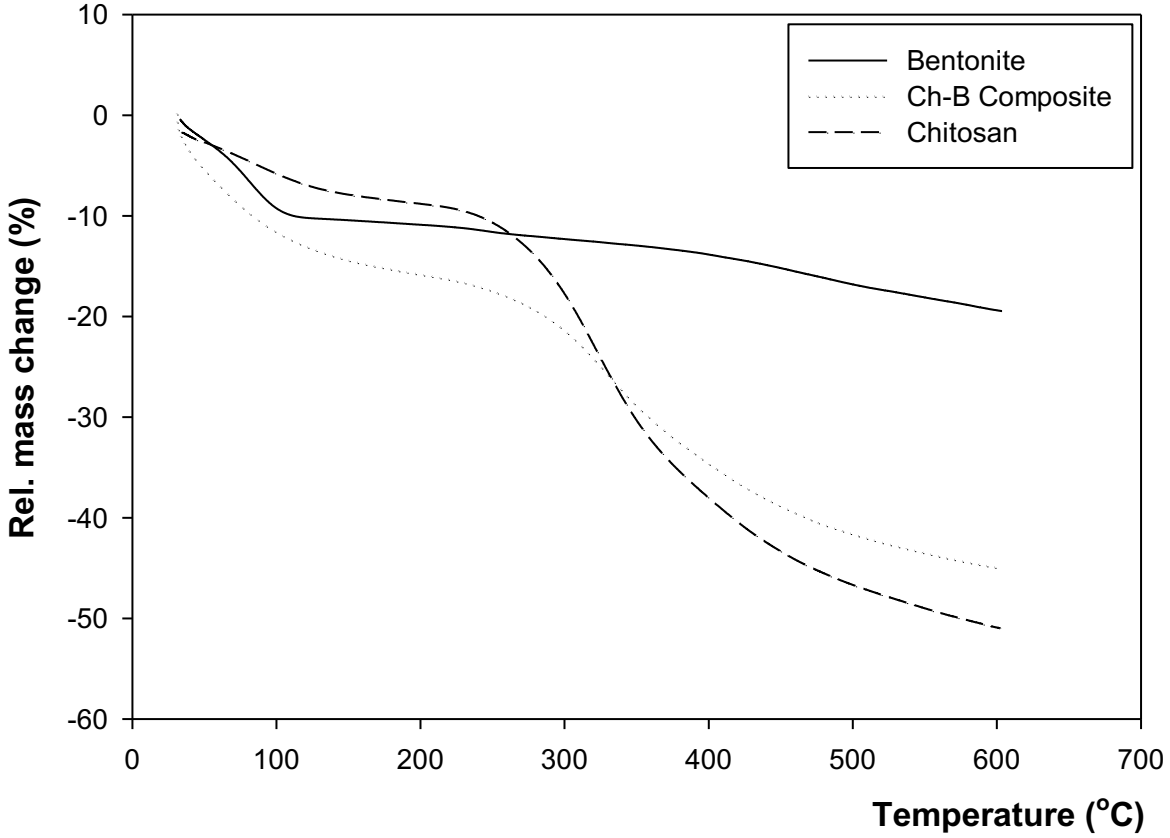

Fig. 2. Thermal gravimetric analysis of Chitosan, Bentonite, and Ch-B Composite

Table 1. Elemental analysis of Chitosan, Bentonite, and Ch-B Composite measured by XRF

Sample	**Chemical composition** (percentage of mass, %)						
	SiO_2	Al_2O_3	Fe_2O_3	CaO	P_2O_5	ZnO	Other
Chitosan	14.0	5.0	25.0	44.9	6.8	1.9	2.4
Bentonite	38.6	11.0	42.1	2.8	0.8	0.1	4.6
Ch-B Composite	27.0	8.6	21.7	37.2	2.5	0.7	2.3

The XRF data provide evidence of the chemical composition of each the adsorbent in Table 1, respectively. It illustrates that the major components are Si, Al, Fe, and Ca. It can only determine the total amount of chemical composition in each sample. These data show that chitosan dominated by Ca, Fe, Si, then Al, bentonite dominated by Fe, Si, Al, then Ca, while the Ch-B dominated by Ca, Fe, Si then Al that seem similar to chitosan but the amount of elements increased when combining with each other. Therefore, these materials of the samples are identical. It illustrates that XRF cannot differentiate between the chemical compositions of the samples, but it can only determine the total amount of Si, Al, Fe, and Ca as a major component in the samples.

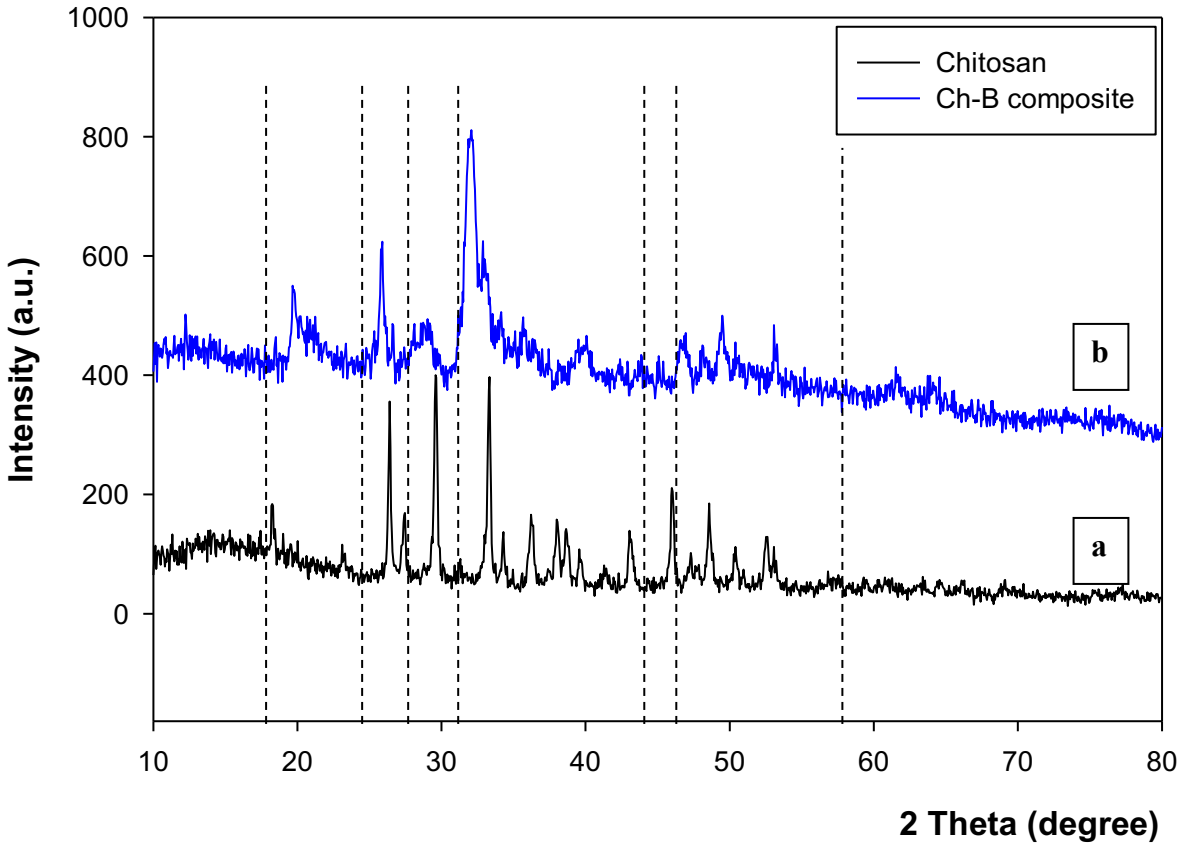

Fig. 3. XRD analysis of (a) Chitosan and (b) Ch-B Composite

XRD patterns of chitosan synthesized from fish scales were observed with their peaks at around 20, 27, 30, 45, 48, 50, and 60° as shown in Fig. 3. It confirmed by the characteristic diffraction including a sharp symmetric strong line at a low value of 2θ, and weaker, less symmetric line at high 2θ values. The major peaks XRD reflections showed in this figure contribute to the formation of chitosan, and these results are matched with the previous reported [15, 17]. The peak at 18° is indicated by the regular crystal lattice of chitosan with a hydrated crystallite structure. XRD pattern of Ch-B composite due to the presence of some minerals from bentonite into the chitosan; some other peaks are also seen broadening at 20 to 50° in the spectra as shown in Fig. 3. Even the bentonite addition causes a decreased in the crystallinity of chitosan [15], the presence of charged groups such as amine, the $-NH_2$, silicate layers on the Ch-B composite leading to electrostatic interaction beside adsorption of turbidity and color removal.

Evaluation of Batch Adsorption Experiments of Contaminated Raw Water

Effect of contact time on the adsorption process

Figure 4 shows that during the first 30 minutes of the adsorption process using Ch-B as the adsorbent, the turbidity concentration decreased significantly from 385 NTU to 200 NTU. It was probably due to the diffusion taking place into the pores and or adsorbed onto the surface of the adsorbent. Initially, all sites on the surface of the adsorbents were vacant and the turbidity concentration gradient was relatively high diffusing into and through the pores of the adsorbent. Afterward, the turbidity concentration slightly decreased to a residual turbidity concentration of 174 NTU (54,81% removal), then finally to be attached to the adsorbent surface, caused by the decrease in the number of vacant sites on the surface of the adsorbent within 4 hours. The time beyond which no significant change in the adsorption occurs has been fixed as the equilibrium time, then can be accepted as the optimum contact time. The adsorption experiments were conducted in 6 hours reaction time for turbidity removal to make sure that the adsorption process is in equilibrium.

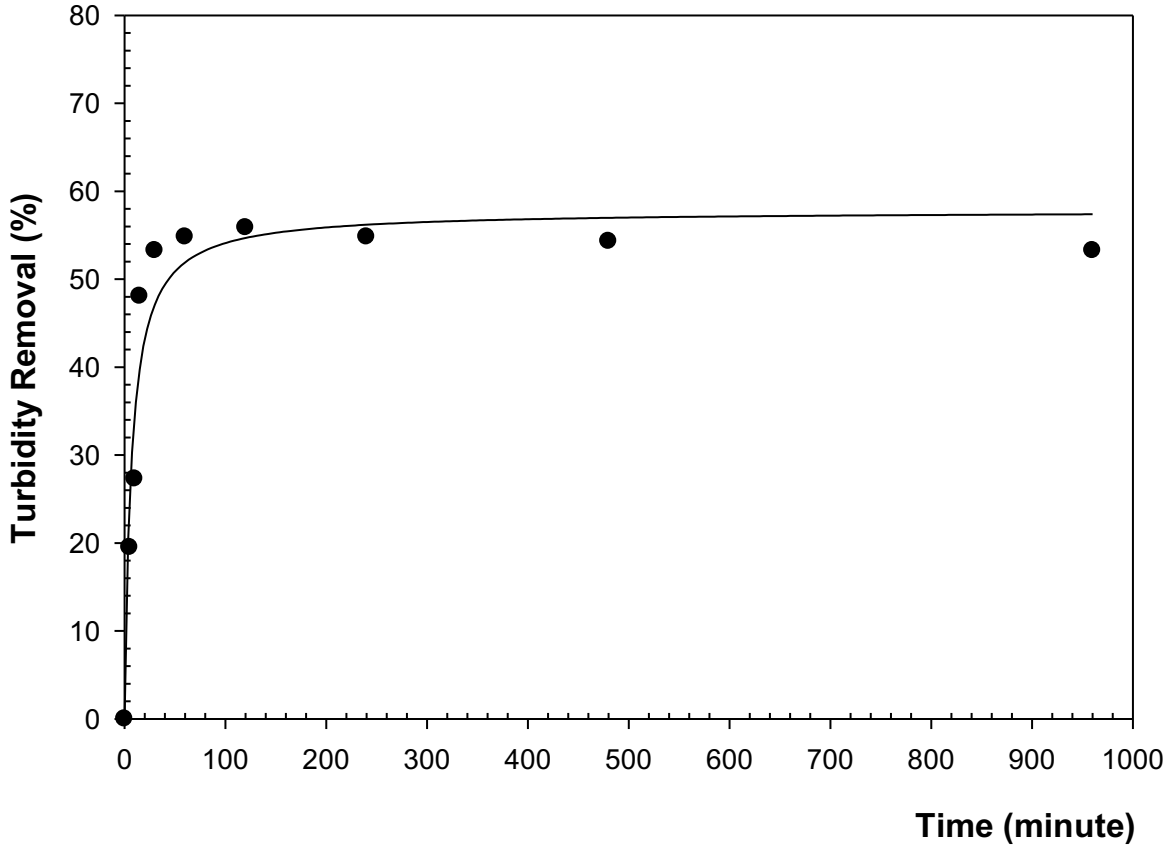

Fig. 4. Effect of contact time on turbidity removal by Ch-B Composite at room temperature, adsorbent dose of 2 g/L, pH_e of 7±0.2, and shaking rate of 150 rpm

Effect of adsorbent dosage for turbidity and color removal on the adsorption process

The most important parameter considered in determining the optimum performance indicator of the adsorbent during the adsorption process is the dosage of the adsorbent in order to minimize costs and obtain the optimum uptake capacity of the contaminant during the treatment process.

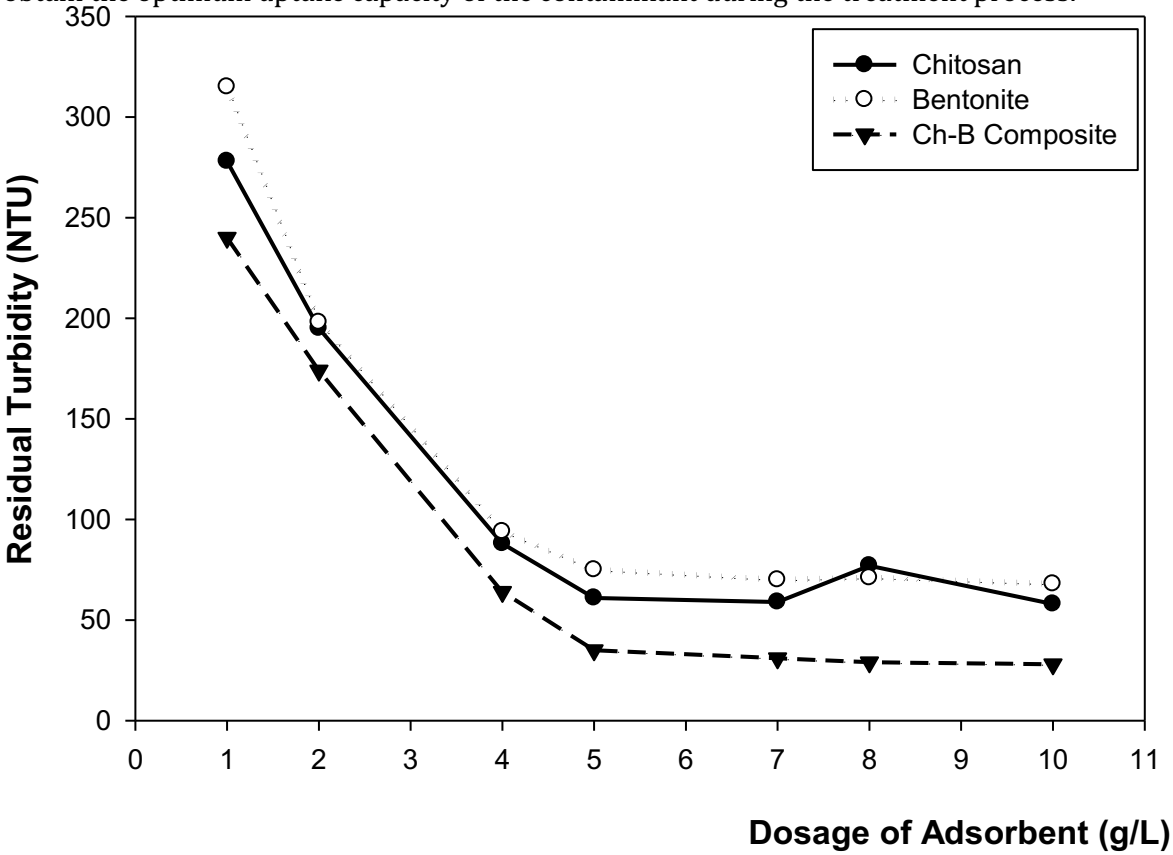

Fig. 5. Effect of adsorbent dosage on turbidity removal when using Chitosan, Bentonite, and Ch-B Composite at room temperature, pH_e of 7±0.2, 150 rpm, 6 h.

The results in Fig. 5 have shown that increased adsorbent dosages lead to better adsorption performance. The adsorbent dosage increases the percentage removal, while keeping all other parameters at a constant value. As the adsorbent dosage increases, the turbidity residual concentration decreases as shown in Fig. 5. At lower adsorbent concentration, the number of active sites is higher. With the increase in adsorbent dosage, aggregation of adsorbent particles would occur in the adsorption process, as a result the removal efficiency increases but the turbidity adsorption capacity decreases as shown in Fig. 6. It occurs because the adsorptive capacity of adsorbent available was not fully utilized at a higher adsorbent dosage in comparison to lower adsorbent dosage. Therefore, it might be possible that the adsorption capacity decreases as the adsorbent dosage increases.

The increase in the adsorbent dose might cause aggregation of adsorbent, and consequently, the available adsorption sites might decrease as well due to the adsorption capacity. With the increase in initial turbidity, the number of colloidal particles in wastewater has increased and thus the number of active sites on the colloidal particles increases for a certain amount of adsorbent [27]. At all initial turbidity values, the turbidity removal efficiency has increased by increasing the dose of the adsorbent. It is because of this issue that by adding the adsorbent into the contaminated water solution, more adsorbent molecules attract solid particles to the active sites and will adsorb them. Shown in Fig. 6, by adding more amount of adsorbent until 10 g/L has no significant effect on turbidity removal compared to 5 g/L of the adsorbent.

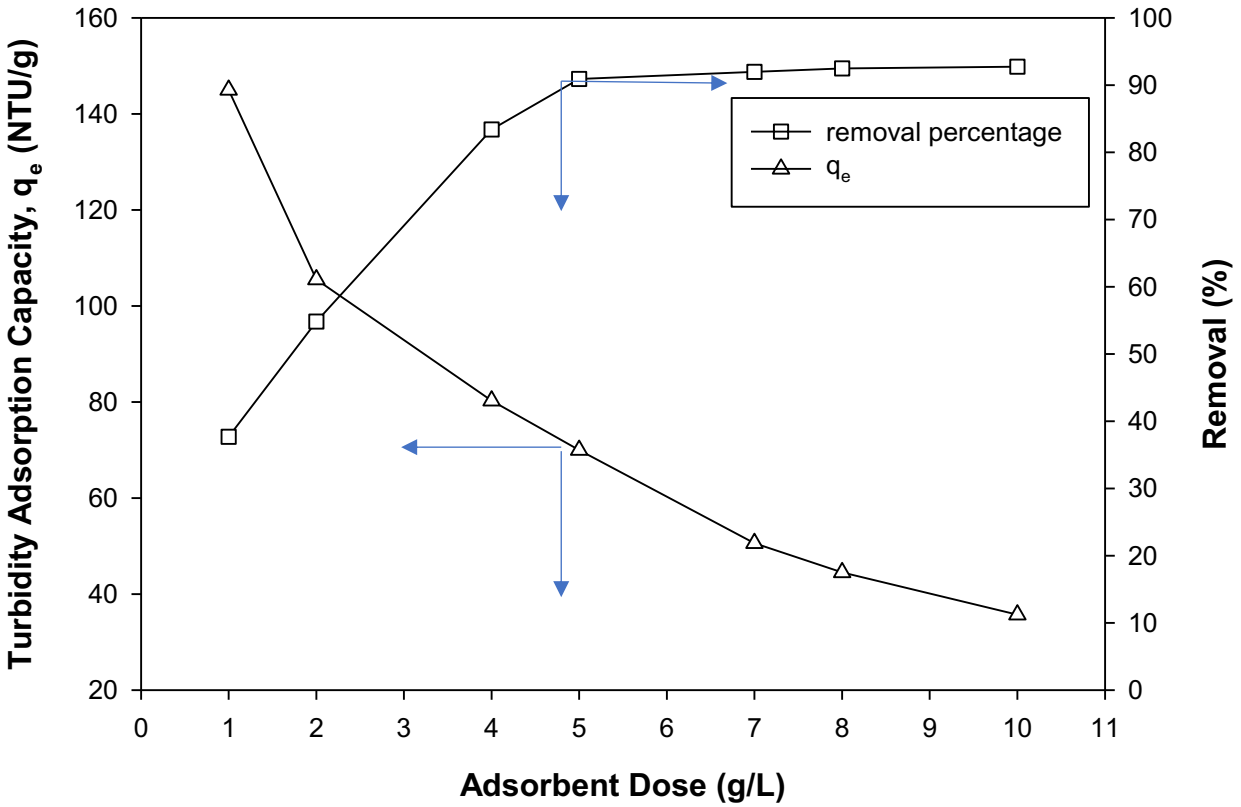

Fig. 6. Effect of adsorbent dosage on turbidity, adsorption capacity and turbidity removal when using Ch-B Composite as adsorbent at room temperature, pH_e of 7±0.2, 150 rpm, 6 h.

Moreover, it is similar observed in Fig. 7 and Fig. 8 that increasing in adsorbent doses to a specific limit (10 g/L), decreased the color concentration residual and increased the removal efficiency, but probably after adding more adsorbent, the residual color will not be changed significantly. The reason was that most of the color removal is happened because of the adsorption process into the pore of adsorbent [28]. With the increase in time adsorption process, the color will cover over the surface of the

adsorbent and after a while, the adsorption locations in the polymer chain of Ch-B composite will be saturated.

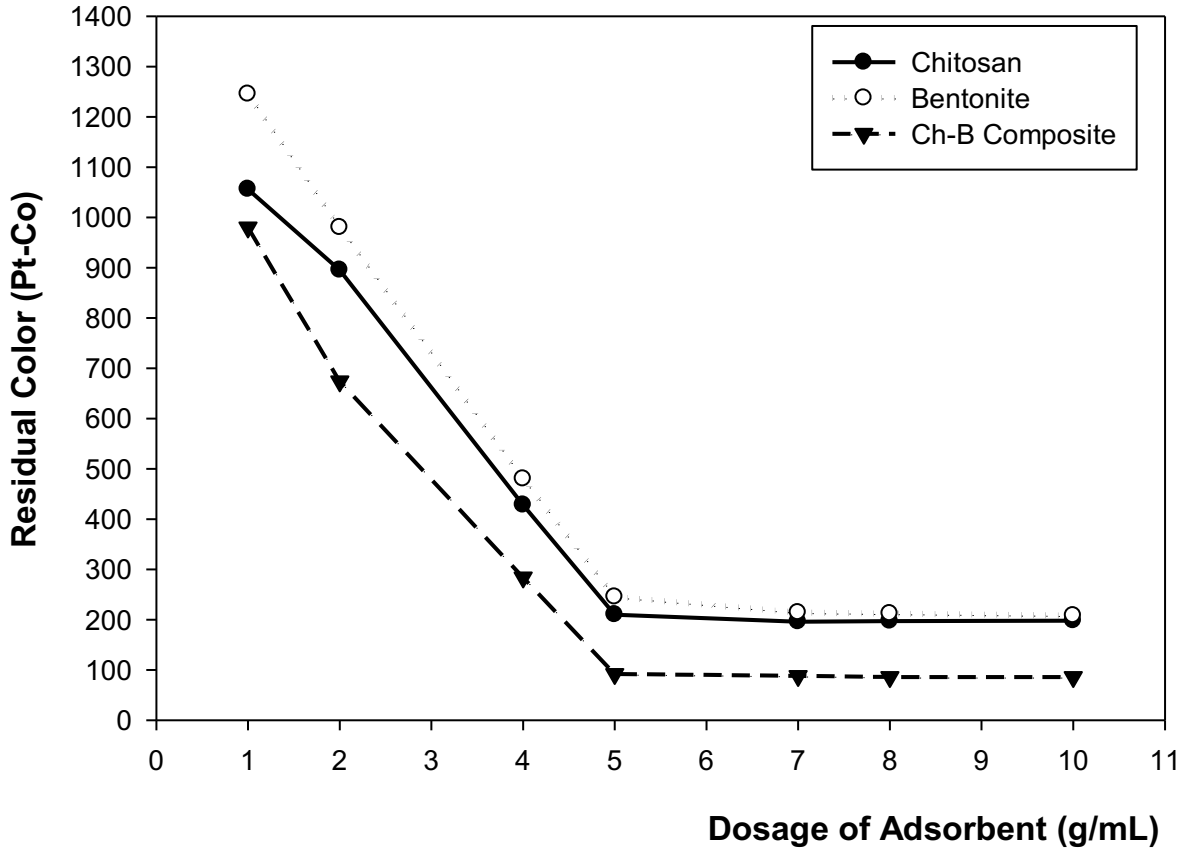

Fig. 7. Effect of adsorbent dosage on color removal when using Chitosan, Bentonite, and Ch-B Composite at room temperature, pH_e of 7±0.2, 150 rpm, 6 h.

The increase of turbidity and color removal can be attributed to the increase of the adsorbent surface area, pores, and active site available for mass transfer, thus more turbidity and color were adsorbed with the increase of adsorbent dosage [29]. It was also the available surface area dependent on adsorbent dosage, however at high adsorbent dosage the available sites of adsorption became higher and hence the removal of color and turbidity is dependent upon adsorbent dosage.

The percentage of adsorption removal increases with increasing amount of adsorbent until a maximum value is reached, and further increase of adsorbent dose does not increase the removal of color and turbidity. The removal percentage of color and turbidity increased with increasing adsorbent dose from 1 g to 10 g in 1 L solution, while the color and turbidity uptake capacity decreased with increasing dose. Low removal percentage at low dose of adsorbent was due to low availability of the adsorption sites. When the adsorbent dose was increased, the available adsorption sites were also increased, resulting in higher color removal. However, increasing the adsorbent dose also resulted in a lower driving force for the adsorbate to diffuse, causing lower adsorption capacity. As shown in Fig. **8**, color removal could not reach 95% even at the highest dose studied. Therefore, it was crucial to determine the optimum dosage, in order to minimize dosing costs and obtain the optimum performance during the treatment.

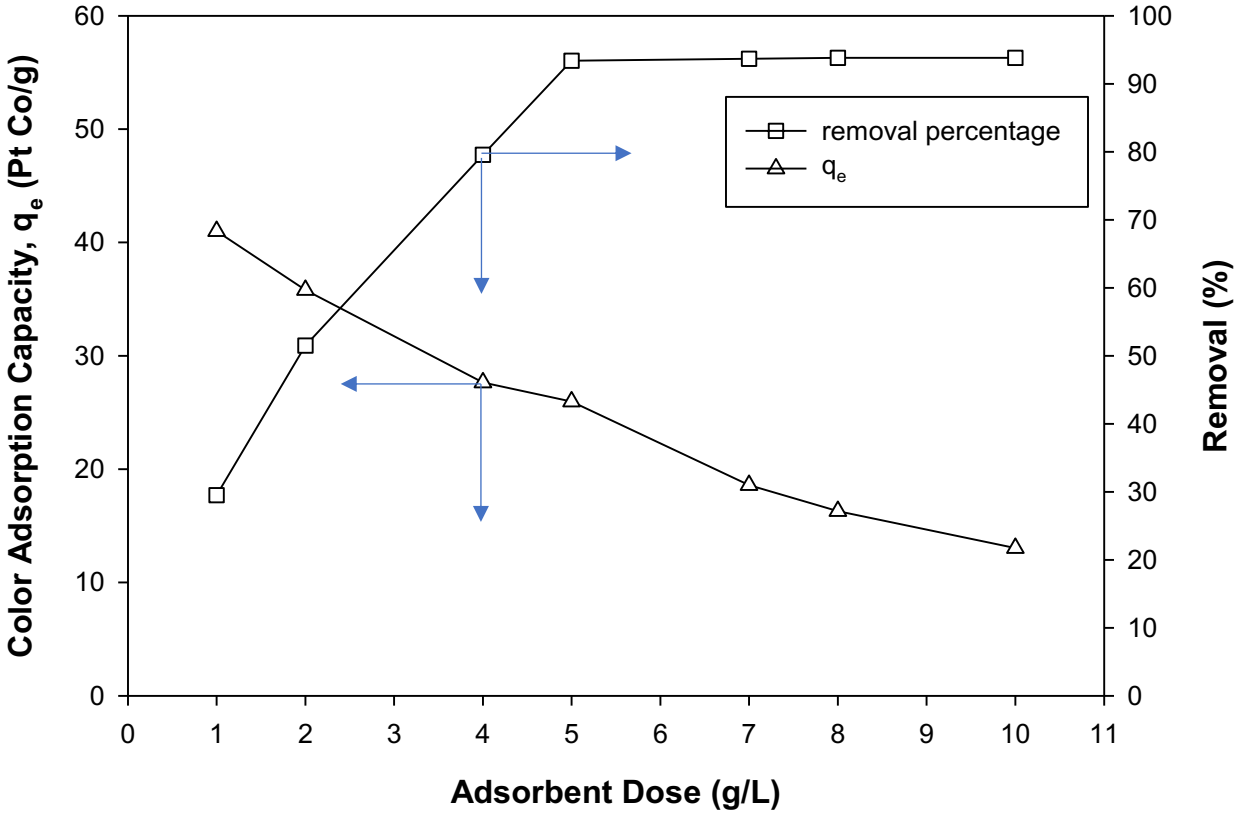

Fig. 8. Effect of adsorbent dosage on color adsorption capacity and color removal when using Ch-B Composite as adsorbent at room temperature, pH_e of 7±0.2, 150 rpm, 6 h.

The composition of the adsorbent such as the amount of alumina present, the amount of silica content, and calcium as shown in Table 1 by XRF analysis contribute to the adsorption of color and turbidity.

Effect of pH equilibrium for turbidity and color removal on the adsorption process

As the pH increased, the percentage of color and turbidity removal decreased. The highest turbidity removal to meet the standard using those adsorbents was observed to occur at pH 7 with a percentage of color removal of 93%, 85%, and 82% and turbidity removal of 90%, 84%, and 80%, respectively, while it is clear that pH changes do alter the final color and turbidity in terms of the overall removal. In comparison, Ch-B exhibits better color and turbidity removal than other adsorbents (**Fig. 9**). Solution pH is always one of the main factors that influence adsorption. Effects of pH on the adsorption of color and turbidity on adsorbents are shown in **Fig. 9 (a) and (b)**. Since the color and turbidity remain permanently ionized over any pH range, its adsorption depends strongly on the pH of the solution that determines the surface charge of the adsorbents. Whenever pH was higher than the pH_{PZC} of the adsorbents (pH_{PZC} of ChB around 6.7±0.2), the adsorption capacity dropped significantly. The surface charge of the adsorbent would be determined from the pH_{PZC} value of the adsorbent; where is its positive surface charge occurs when pH solution is lower than pH_{PZC} and vice versa [30–32].. Overall, lower pH was favorable for adsorption of color and turbidity. There was practically small adsorption occurring when the pH was shifted to pH higher than pH_{PZC} of each adsorbent. The effect of pH on color and turbidity adsorption suggested that the electrostatic interaction was the main driving force for the adsorption.

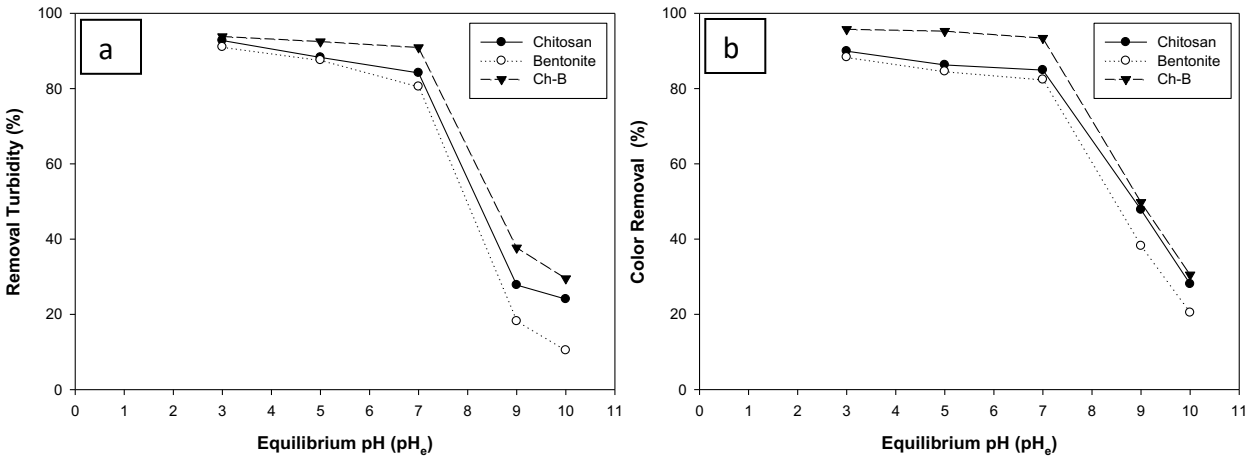

Fig. 9. Effect of equilibrium pH (pH_e) on turbidity removal (a) and color removal (b) using Chitosan, Bentonite, and Ch-B Composite as adsorbent at room temperature, dosage of 5 g/L, 150 rpm, 6 h.

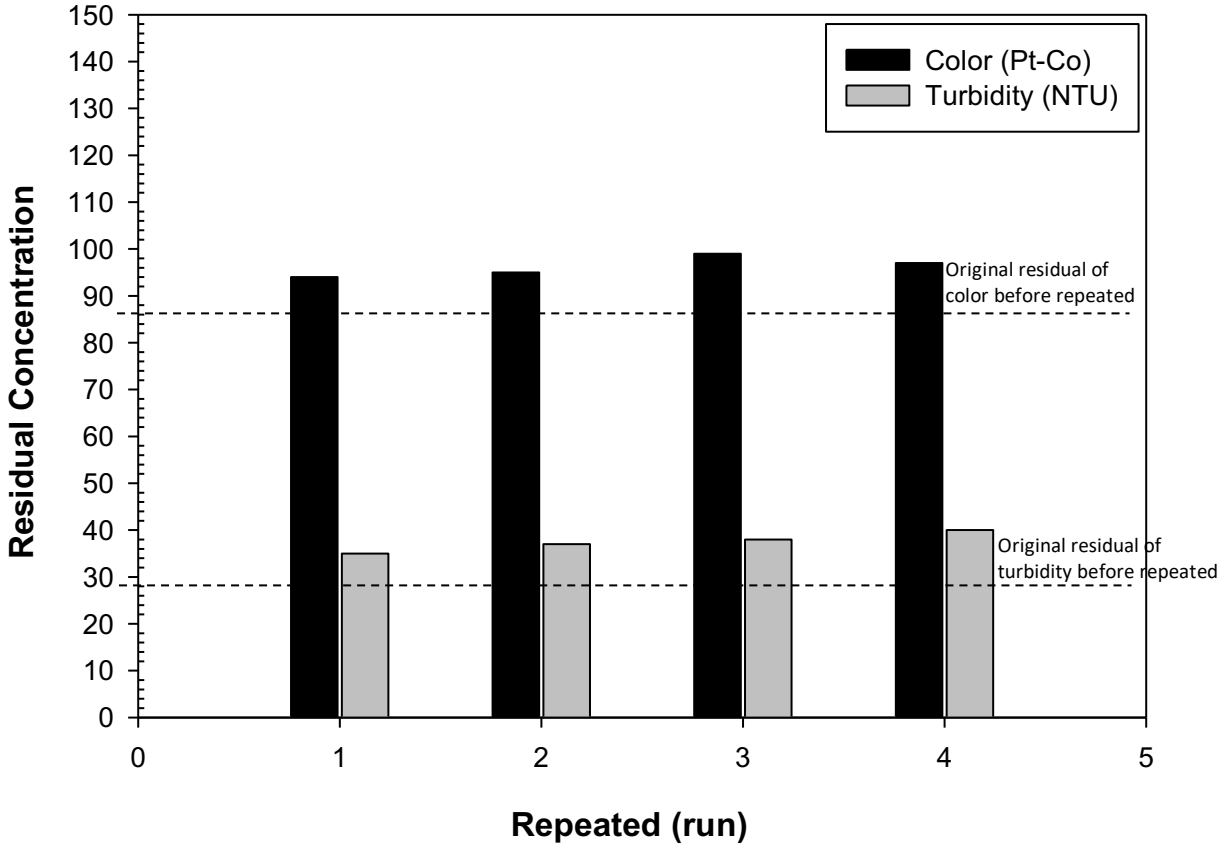

Fig. 10. Residual concentration for turbidity (NTU) and color (Pt-Co) adsorption using Ch-B composite as adsorbent during 4 repeated at room temperature, Ch-B composite dose of 5 g/L, pH_e of 7±0.2, 150 rpm, 6 h.

The Ch-B composite was regenerated successfully without significantly reducing its adsorption capacity. The recovered Ch-B composite was kept in 0.01 N HCl with vigorous stirring for 24 h. The activity of the recovered Ch-B composite was slightly lower than that observed in the 1st reaction. It is around 11% uptake capacity decrease was observed after the repetition (Fig. 10). These results indicate

that the turbidity and color can be adsorbed on Ch-B composite and the adsorption performance has not significantly deteriorated in the course of adsorption runs.

4. Conclusions

Chitosan–bentonite composite (Ch-B composite) has been successfully synthesized. It was characterized by Fourier transform infrared spectroscopy (FTIR), scanning electron microscopy (SEM), and X-ray Fluorescence (XRF) and X-ray Diffraction (XRD) analysis. XRF and EDX analysis confirmed the existence of Si, Al, Fe and Ca. These composites were used for the treatment of contaminated raw water sources as adsorbents. Batch experiment adsorption process using the composite of chitosan-bentonite (Ch-B) for treating raw source water was significant to reduce the value of turbidity and color becomes 24.8±2 NTU and 86.7±5 Pt-Co, respectively. The results then compare to the treatment using the commercial chitosan and bentonite self. The highest removal uptake capacities for this process using Ch-B as adsorbent were 90.20% for turbidity removal and 93.14% for color removal which were obtained in optimum dosage conditions of 5 g/L. Moreover, it its found that the raw water treatment using the composite of chitosan-bentonite is favorable than chitosan and bentonite materials. The Ch-B can be considered as an appropriate adsorbent for turbidity and color removal from contaminated source water. These Ch-B composites were being safe for human health, biodegradable, and absence of toxicity as a natural adsorbent.

Acknowledgments

This work was financially supported by a grant of Directorate of Research and Community Service, Ministry of Research, Technology and Higher Education of Indonesia, and the fund for Applied Research University Grant.

Conflict of Interest

The authors declare no conflict of interest in this research.

References

Price, J. I., & Heberling, M. T. The Effects Of Source Water Quality On Drinking Water Treatment Costs: A Review And Synthesis Of Empirical Literature. Ecological Economics, 151, 195. 2018

Aboubaraka, A. E., Aboelfetoh, E. F., & Ebeid, E.-Z. M. Coagulation Effectiveness Of Graphene Oxide For The Removal Of Turbidity From Raw Surface Water. Chemosphere, 181, 738. 2017

Gitis, V., & Hankins, N. Water Treatment Chemicals: Trends And Challenges. Journal Of Water Process Engineering, 25, 34. 2018

Irawan, C., Ramadhan, M. W., Nata, I. F., & Putra, M. D. The Treatment Of Raw Water Sources Of Drinking Water Using Chitosan/Mg/Al–Ldh Composites: Problem Cases In Municipal Waterworks In Banjarmasin. Iop Conference Series: Earth And Environmental Science, 506(1), 12003. 2020

Hassan, M. S., Nikman, K. A., & Ahmad, F. Removal Of Methylene Blue From Aqueous Solution Using Cocoa (Theobroma Cacao) Nib-Based Activated Carbon Treated With Hydrochloric Acid. Malaysian Journal Of Fundamental And Applied Sciences, 14(2), 5. 2018

Arshad, S. H. M., Ngadi, N., Wong, S., Amin, N. S., Razmi, F. A., Mohamed, N. B., … Aziz, A. A. Optimization Of Phenol Adsorption Onto Biochar From Oil Palm Empty Fruit Bunch (Efb). Malaysian Journal Of Fundamental And Applied Sciences , 15(1), 5. 2019

Bonfante-Alvarez, H., Avila-Montiel, G. De, Herrera-Barros, A., Torrenegra-Alarcón, M., & Delgado, Á. D. G. Evaluation Of Five Chitosan Production Routes With Astaxanthin Recovery From Shrimp Exoskeletons. Chemical Engineering Transactions, 70, 1969. 2018

Chen, L., Wu, P., Chen, M., Lai, X., Ahmed, Z., Zhu, N., … Liu, T. Preparation And Characterization Of The Eco-Friendly Chitosan/Vermiculite Biocomposite With Excellent Removal Capacity For Cadmium And Lead. Applied Clay Science, 159, 74. 2018

Zafar, R., Zia, K. M., Tabasum, S., Jabeen, F., Noreen, A., & Zuber, M. Polysaccharide Based Bionanocomposites, Properties And Applications: A Review. International Journal Of Biological Macromolecules, 92, 1012. 2016

Sadiana, I., Karelius, K., Agnestisia, R., & Fatah, A. Studies On Synthesis, Characterization, And Adsorption Of Cationic Dyes From Aqueous Solutions Using Magnetic Composite Material From Natural Clay In Central Kalimantan, Indonesia. Molekul, 13, 63. 2018

Wang, J., & Chen, C. Chitosan-Based Biosorbents: Modification And Application For Biosorption Of Heavy Metals And Radionuclides. Bioresource Technology, 160, 129. 2014

Azzam, E. M. S., Eshaq, G., Rabie, A. M., Bakr, A. A., Abd-Elaal, A. A., El Metwally, A. E., & Tawfik, S. M. Preparation And Characterization Of Chitosan-Clay Nanocomposites For The Removal Of Cu(Ii) From Aqueous Solution. International Journal Of Biological Macromolecules, 89, 507. 2016

Zemmouri, H., Drouiche, M., Sayeh, A., Lounici, H., & Mameri, N. Chitosan Application For Treatment Of Beni-Amrane's Water Dam. Energy Procedia, 36, 558. 2013

Vakili, M., Rafatullah, M., Salamatinia, B., Abdullah, A. Z., Ibrahim, M. H., Tan, K. B., … Amouzgar, P. Application Of Chitosan And Its Derivatives As Adsorbents For Dye Removal From Water And Wastewater: A Review. Carbohydrate Polymers, 113, 115. 2014

Giannakas, A., Grigoriadi, K., Leontiou, A., Barkoula, N.-M., & Ladavos, A. Preparation, Characterization, Mechanical And Barrier Properties Investigation Of Chitosan–Clay Nanocomposites. Carbohydrate Polymers, 108, 103. 2014

Chang, S.-H., Wang, K.-S., Chang, W.-C., Tu, C.-C., Chen, H.-J., Chang, C.-Y., & Jeng, R.-S. Screening Long-Time Plating Effluent Qualities By Sorbent Sorption With Xrf Analysis. Journal Of Hazardous Materials, 138(1), 67. 2006

Kumari, S., Kumar Annamareddy, S. H., Abanti, S., & Kumar Rath, P. Physicochemical Properties And Characterization Of Chitosan Synthesized From Fish Scales, Crab And Shrimp Shells. International Journal Of Biological Macromolecules, 104, 1697. 2017

Sarode, S., Upadhyay, P., Khosa, M. A., Mak, T., Shakir, A., Song, S., & Ullah, A. Overview Of Wastewater Treatment Methods With Special Focus On Biopolymer Chitin-Chitosan. International Journal Of Biological Macromolecules, 121, 1086. 2019

Yen, M.-T., Yang, J.-H., & Mau, J.-L. Physicochemical Characterization Of Chitin And Chitosan From Crab Shells. Carbohydrate Polymers, 75(1), 15. 2009

Lewandowska, K., Sionkowska, A., Kaczmarek, B., & Furtos, G. Characterization Of Chitosan Composites With Various Clays. International Journal Of Biological Macromolecules, 65, 534. 2014

Chao, L., Wang, Y., Chen, S., & Li, Y. Preparation And Adsorption Properties Of Chitosan-Modified Magnetic Nanoparticles For Removal Of Mo (Vi) Ions. Polish Journal Of Environmental Studies, 30(3), 2489. 2021

Syafalni Abustan, Ismail, Zakaria, Siti Nor Farhana, Zawawi, Mohd Hafiz, Rahim, Rafini Abd, S. Raw Water Treatment Using Bentonite-Chitosan As A Coagulant. Water Science And Technology: Water Supply, 12(4), 480. 2012

Ayub, N., & Chaudhry, M. N. Efficiency Of Aluminium Pillared Montmorillonite Clays Of Pakistani Origin (Peshawar And Samwal) On The Adsorption Of Chromium Ions In Aqueous Solutions. Polish Journal Of Environmental Studies, 30(2), 1039. 2021

Bougdah, N., Messikh, N., Bousba, S., Magri, P., Djazi, F., & Zaghdoudi, R. Adsorption Of Humic Acid From Aqueous Solution On Different Modified Bentonites . Chemical Engineering Transactions, 60, 223. 2017

Kumari, S., Rath, P., Sri Hari Kumar, A., & Tiwari, T. N. Extraction And Characterization Of Chitin And Chitosan From Fishery Waste By Chemical Method. Environmental Technology & Innovation, 3, 77. 2015

Lewandowska, K., Sionkowska, A., Kaczmarek, B., & Furtos, G. Characterization Of Chitosan Composites With Various Clays. International Journal Of Biological Macromolecules, 65, 534. 2014

Syafalni Abustan Ismail Zakaria Siti Nor Farhana Zawawi Mohd Hafiz Rahim Rafini Abd, S. Raw Water Treatment Using Bentonite-Chitosan As A Coagulant. Water Science And Technology: Water Supply, 12(4), 480. 2012

Vakili, M., Rafatullah, M., Salamatinia, B., Abdullah, A. Z., Ibrahim, M. H., Tan, K. B., … Amouzgar, P. Application Of Chitosan And Its Derivatives As Adsorbents For Dye Removal From Water And Wastewater: A Review. Carbohydrate Polymers, 113, 115. 2014

Saadon, S. A., Yunus, S. M., Yusoff, A. R., Yusop, Z., Azman, S., Uy, D., & Syafiuddin, A. Heated Laterite As A Low-Cost Adsorbent For Arsenic Removal From Aqueous Solution. Malaysian Journal Of Fundamental And Applied Sciences, 14(1), 8. 2018

Lu, Y., Liu, X., Yu, L., Zhang, X., Duan, W., Park, J., & Dong, X. Removal Characteristics And Mechanism Of Mn(Ii) From Acidic Wastewater Using Red Mud-Loess Mixture. Polish Journal Of Environmental Studies. 2022

Angkawijaya, A. E., Santoso, S. P., Bundjaja, V., Soetaredjo, F. E., Gunarto, C., Ayucitra, A., … Ismadji, S. Studies On The Performance Of Bentonite And Its Composite As Phosphate Adsorbent And Phosphate Supplementation For Plant. Journal Of Hazardous Materials, 399, 123130. 2020

Zyoud, A. H., Zubi, A., Zyoud, S. H., Hilal, M. H., Zyoud, S., Qamhieh, N., … Hilal, H. S. Kaolin-Supported Zno Nanoparticle Catalysts In Self-Sensitized Tetracycline photodegradation: Zero-point charge and pH effects. Applied Clay Science, 182, 105294. 2019